Numerical Simulation and Experimental Verification of the Influence of Channel Structure on Multiphase Heat and Mass Transfer in Chip Cooling

Chenxuan Wang*

School of Energy and Electrical Engineering, Chang'an University, Xi'an, China

*Corresponding author: ChenXuan_Wang26@126.com

Abstract. With the continuous improvement of chip integration and power density, traditional air cooling technology has struggled to meet the heat dissipation requirements in high heat flux density scenarios. This study investigates the influence of channel structures on multiphase heat and mass transfer in chip cooling. A three-dimensional simulation model of an IGBT module and its cooling channel was established. Numerical simulations of heat and mass transfer characteristics for rectangular, trapezoidal, and circular cross-section channel structures were conducted using ANSYS FLUENT software. An experimental platform was also built to verify the heat dissipation performance. The results show that under the same cross-sectional area and flow velocity, the maximum temperature on the heat source surface of the circular cross-section microchannel is significantly lower than that of the rectangular and trapezoidal cross-sections, with reductions of 3.8–5.3 °C and 2.2–2.9 °C, respectively. Its Nusselt number (11.63) is also significantly higher than that of the rectangular (8.58) and trapezoidal (8.90) sections, indicating the strongest convective heat transfer capability. The circular cross-section enhances heat transfer due to more uniform fluid distribution and thinner boundary layers, but its processing difficulty and flow resistance need to be balanced. The heat transfer performance of trapezoidal and rectangular sections is similar, but the rectangular section is more easily implemented in engineering applications due to its simple structure. This study provides a theoretical basis and practical reference for the optimized design of high-power density chip radiators.

Keywords: Multiphase Heat and Mass, Chip Cooling, Microfluidic Channel.

1. Introduction

As chip integration and power density continue to increase, traditional air cooling technologies have become insufficient to address heat dissipation challenges in high heat flux density scenarios[1]. To overcome this bottleneck, researchers have proposed advanced cooling technologies such as jet cooling, electro-thermal cooling, and heat pipe cooling. However, these technologies generally suffer from lengthy heat transfer paths, and the thermal resistance of multi-layer interfaces significantly restricts the improvement of heat dissipation capacity[2]. Therefore, embedded cooling methods have been proposed, which effectively address the high heat flux density problem of electronic chips by eliminating thermal interface materials (TIM). Among them, channel liquid cooling technology has become the core solution for chip heat dissipation due to its high efficiency, low energy consumption, and compact structure[3].

In the heat dissipation process, multiphase flow exhibits great potential in high heat flux density cooling due to its unique phase change heat transfer characteristics. In a channel liquid cooling system, the coolant flows through the channel to absorb heat generated by the chip. When the heat flux density exceeds a critical value, the coolant undergoes phase change, generating bubbles and forming a gas-liquid two-phase flow pattern. It is noteworthy that the design of the chip cooling channel structure has a decisive influence on the heat and mass transfer process of multiphase flow. Different channel structure parameters (such as cross-sectional shape, geometric dimensions, arrangement, etc.) significantly alter the flow pattern distribution, velocity field characteristics, and phase change position and intensity of multiphase flow, thereby affecting the heat and mass transfer efficiency[4].

This paper establishes a three-dimensional simulation model of an IGBT module and its cooling channel[5]. Using ANSYS FLUENT software, numerical simulations and analyses were performed on key performance parameters such as heat transfer efficiency and power consumption of the IGBT module in the power control system, with a focus on exploring the influence laws of different channel structures on the heat and mass transfer characteristics of multiphase flow[6]. Meanwhile, an experimental test platform for the IGBT module radiator was built to systematically detect and evaluate its heat dissipation performance, providing a theoretical basis and practical reference for the optimized design of power module radiators.

2. Research Methods and Model Construction

The research object in this paper is an Infineon ICBT module, where the IGBT chip size is 10 mm × 10 mm × 0.7 mm; the uniform heat source layer is 10 mm × 10 mm with a thickness of 0.012 mm; the base cold plate size is 50 mm × 50 mm × 0.7 mm; there is one inlet and one outlet for the channel, with a cross-section of 0.5 mm × 0.25 mm. The inlet and outlet of the coolant flow are both horizontal, ensuring uniform coolant flow. The IGBT module was modeled and analyzed using the 3D modeling software SolidWorks[7], and simulation parameters were set using Fluent software for numerical simulation. A sample of the modeling structure is shown in Figure 1(a).

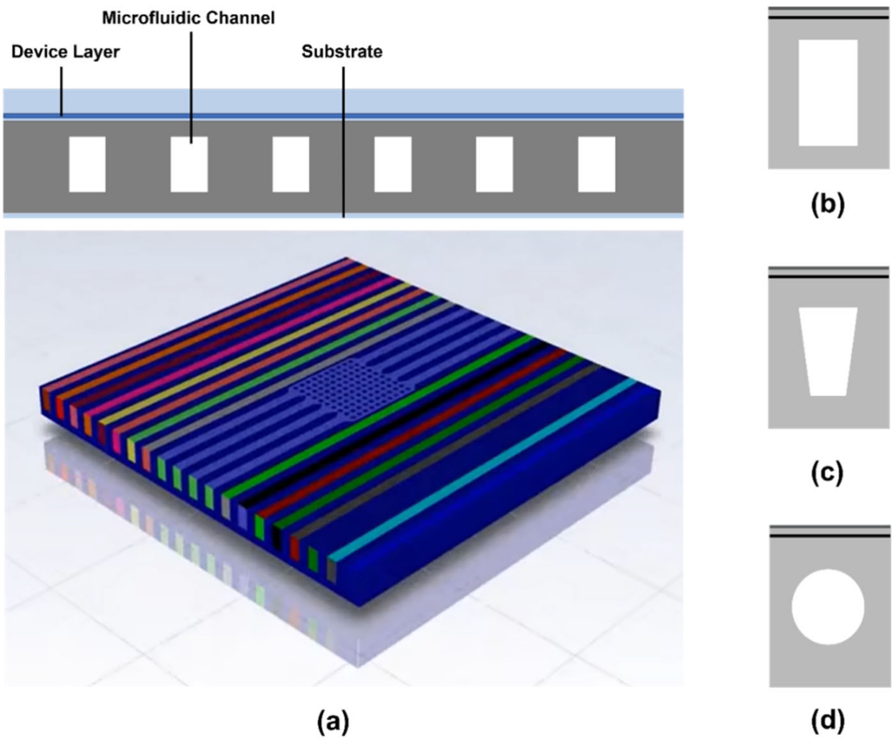

Figure 1. (a) Simulation model principle and modeling (b) Rectangular cross section (c) Trapezoidal cross section (d) Circular cross section

Figure 1 includes different microchannel structures with the same cross-sectional area. The rectangular microchannel in (b) has a cross-sectional size of 0.125 mm × 0.25 mm, the trapezoidal microchannel in (c) has a cross-sectional size of (0.1 mm + 0.15 mm) × 0.25 mm, and the circular microchannel in (d) has a cross-sectional size of R = 0.09974 mm. Since different working fluids have different physical parameters, which can significantly affect the oscillation characteristics and heat transfer performance of microchannels, in the process of solving the simulation model using FLUENT simulation software, the heat source layer uses equivalent materials, the substrate layer uses material Si, and water and acetone are used as simulation working fluids. Their detailed physical properties are shown in Table 1.

Table 1. Material Properties of Simulation Models

Name	Material	Density	Specific heat capacity	Thermal conductivity
Substrate	Si	2329 kg/m^3	700 J/kg•K	150 W/m•K
Heat source layer	Equivalent material	5 kg/m^3	517 J/kg•K	2.25 W/m•K
Industrial quality	Water	998.2 kg/m^3	4182 J/kg•K	0.6 W/m•K
Industrial quality	Acetone	744 kg/m^3	2290 J/kg•K	0.168 W/m•K

In this design, water and acetone are used as the working fluids for the microchannel, the pipeline is in a horizontal state, and the influence of the gravitational field is not considered. The VOF model is used to track the phase interface, and the Lee model is used to simulate the evaporation-condensation process. The gas phase is defined as the first phase, and the liquid phase is defined as the second phase. In the setup, the boundary conditions are mainly set for the evaporation end, condensation end, and adiabatic end of the microchannel: the condensation end is kept at a constant 26.85 °C, the adiabatic end is set as an adiabatic boundary, and the evaporation end is defined by the heat flux value, with a selection range of 1 W/cm^2 to 20 W/cm^2. Before the simulation calculation, to exclude the influence of grid size on simulation accuracy, a grid independence verification is required. Three unit grid sizes of 8 μm, 6 μm, and 4 μm were used to divide the grid of the simulation model. After average flow velocity testing, considering both simulation calculation accuracy and efficiency, a 6 μm grid size was selected for the grid meshing and research of the micro pulsating heat pipe in this paper.

Finally, the solution of the simulation model is carried out. When FLUENT performs internal calculations, the model is first meshed to generate calculation nodes. Secondly, the control equations of fluid mechanics, including the continuity equation, mass conservation equation, and momentum conservation equation, are applied to the calculation nodes, in which the mass source terms in the control equations are solved in combination with the evaporation-condensation model. This process mainly involves constructing discrete equations within the software, solving the equations by combining discrete initial conditions and boundary conditions. If the equations can converge, the results at that moment are output for iterative calculation; if not, discrete equations are reconstructed for calculation.

3. Results

The result analysis is based on the fundamental laws of thermodynamics, and energy conservation is a classic thermodynamic law. During fluid flow, the entire fluid system exchanges energy with the outside world. Energy from the outside enters the system, and energy inside the system is transferred to the outside. The energy entering the fluid micro-element plus the work done by the forces acting on the micro-element equals the increase in energy within the micro-element, with the total energy remaining constant throughout the process. The equation is:

$$C_v \frac{dT}{dt} + \nabla \cdot \left(-k_f \nabla T\right) + C_v \overrightarrow{v \cdot \nabla T} = P \tag{1}$$

The Nusselt number (Nu), named after the German physicist Wilhelm·Nusselt, represents a dimensionless number for the intensity of convective heat transfer. It is the ratio of the thermal conduction resistance of the fluid laminar sublayer to the convective heat transfer resistance, i.e., the normalized temperature gradient at the solid-fluid contact interface. A larger Nusselt number corresponds to more active convection. The formula for the Nusselt number is:

$$Nu_{fd} = \frac{h_f D_h}{k_f} \tag{2}$$

Under the conditions of equal cross-sectional area and a fluid inlet velocity of 1.0 m/s, the temperature distribution maps of the heat source surface for rectangular, trapezoidal, and circular cross-section microchannels during heat dissipation were simulated, as shown in Figure 2. The distribution map is mainly composed of two parts: the temperature map (left) and the color legend (right), where different colors on the heat source surface in the temperature map represent different temperatures. The temperature range refers to the color legend, with blue indicating low temperature and red indicating high temperature. In the following simulation diagrams, the fluid inlet is on the right side of the temperature distribution map, and the outlet is on the left side, with the fluid flowing in the negative X-axis direction. The liquid temperature at the inlet is set to room temperature of 20 °C, which is shown as the lowest temperature (blue) in the heat source surface temperature distribution. The temperature gradually increases from the inlet to the outlet, with the highest temperature (red) at the outlet. Since the maximum temperature in each temperature distribution map is different, and the minimum temperature is 20 °C, the temperature represented by the color legend in each temperature distribution map varies slightly, requiring temperature analysis according to the corresponding color legend for each map.

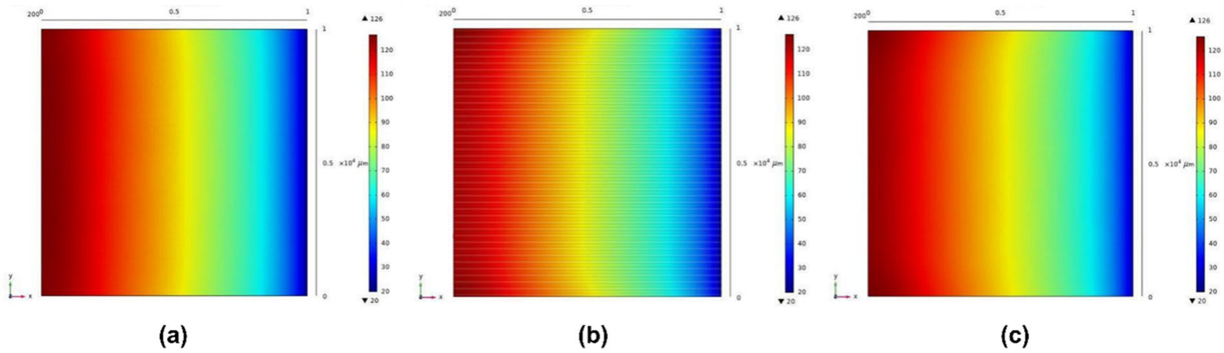

Figure 2. Temperature profile (a) Rectangular (b) Trapezoidal (c) Circular

When the cross-sectional area is constant, the maximum temperature distribution on the heat source surface of the circular cross-section microchannel is lower than that of the rectangular and trapezoidal cross-sections. The maximum temperature of the circular cross-section microchannel for heat dissipation is 2.2 °C to 2.9 °C lower than that of the trapezoidal cross-section and 3.8 °C to 5.3 °C lower than that of the rectangular cross-section under the same velocity. This is because, with a constant cross-sectional area (equal flow rate for each cross-section), the spacing between circular cross-section microchannels is 48 μm, which is smaller than the spacing of rectangular and trapezoidal cross-sections. That is, the advantage of circular microchannels is that they occupy more space in the Y-direction distribution of the three-dimensional cross-section. Therefore, when the cross-sectional area is constant (equal flow rate), circular cross-sections have better heat dissipation effects than rectangular and trapezoidal cross-section microchannels.

Under the same flow velocity (1 m/s), the Nusselt number of the circular cross-section (11.63) is significantly higher than that of the rectangular (8.58) and trapezoidal (8.90) sections, indicating the strongest convective heat transfer capability. This result is consistent with the temperature distribution simulation conclusion (the circular cross-section has the lowest maximum temperature) because the circular cross-section has more uniform fluid distribution and a thinner boundary layer, enhancing the heat transfer effect. Although the Nu value of the trapezoidal cross-section is slightly higher than that of the rectangular cross-section, the difference is small (8.90 vs. 8.58), mainly because the hydraulic diameter of the trapezoidal cross-section is close to that of the rectangular cross-section, but the complexity of the fluid flow path slightly improves the heat transfer efficiency. However, the

Nu advantage of the circular cross-section is significant, but it should be noted that it has a higher pressure drop (the circular pressure drop is 5.81 kPa, the rectangular is 5.81 kPa, and the trapezoidal is 5.81 kPa, but there may be slight differences due to flow resistance in reality). In summary, the circular cross-section has the best heat transfer performance, but its processing difficulty and flow resistance need to be balanced. The trapezoidal and rectangular cross-sections have similar heat transfer capabilities, but the rectangular cross-section is more practical in engineering due to its easier processing.

4. Conclusions

Simulation and experimental results show that the channel cross-sectional shape directly affects the bubble generation position, flow pattern distribution, and phase change intensity. The compact layout of the circular cross-section helps enhance phase change heat transfer efficiency, but its stability under complex flow conditions requires further study. Under the same flow rate, the circular cross-section microchannel exhibits the strongest convective heat transfer capability due to better fluid distribution and a thinner boundary layer, effectively reducing the temperature of the heat source surface. In contrast, rectangular and trapezoidal cross-sections have weaker heat transfer performance, but their simple structures make them more suitable for practical engineering scenarios. Although the circular cross-section dominates in heat transfer performance, its higher processing difficulty and possible larger pressure drop require optimized design according to specific application scenarios. For engineering needs that require balancing performance and cost, trapezoidal or rectangular cross-sections can be more practical choices. Follow-up research can further explore the influence of asymmetric channel structures and multi-working fluid mixed cooling on multiphase heat transfer, and optimize channel geometric parameters by combining artificial intelligence algorithms to achieve high efficiency and intelligence of chip cooling systems.

References

[1] L. Chen, H. Xu, X. Sun and Y. Cai. Three-Vector-Based Model Predictive Torque Control for a Permanent Magnet Synchronous Motor of EVs[J]. IEEE Transactions on Transportation Electrification, 2021, pp. 1454-1465.

[2] D. Sekar et al. A 3D-IC Technology with Integrated Microchannel Cooling[C]. 2008 International Interconnect Technology Conference, Burlingame, CA, USA, 2008, pp. 13-15.

[3] Bing Dang, P. Joseph, M. Bakir, T. Spencer, P. Kohl and J. Meindl. Wafer-level microfluidic cooling interconnects for GSI[C]. Proceedings of the IEEE 2005 International Interconnect Technology Conference, 2005., Burlingame, CA, USA, 2005, pp. 180-182.

[4] Fubo Xie, Xinlong Li, Peng Qian, Zizhen Huang, Minghou Liu. Effects of geometry and multisource heat input on flow and heat transfer in single closed-loop pulsating heat pipe[J]. Applied Thermal Engineering, 2020,114856: 1359-4311.

[5] Han L, Liang L, Kang Y, et al. A review of SiC IGBT: models, fabrications, characteristics, and applications[J]. IEEE Transactions on Power Electronics, 2020, 36(2): 2080-2093.

[6] Shabani S, Majkut M, Dykas S, et al. Numerical analysis of the condensing steam flow by means of ANSYS fluent and in-house academic codes with respect to the capacity for thermodynamic assessment[J]. Frontiers in Energy Research, 2022, 10: 902629.

[7] Dong W, Meng X, Song X, et al. IGBT radiator design and simulation[J]. Journal of System Simulation, 2020, 28(9): 2095-2100.